THE INFLUENCE OF AGING HEAT TREATMENTS ON THE STRUCTURAL AND MECHANICAL CHARACTERISTICS OF ALUMINUM ALLOY 2017A

Andreea Daniela BUZATU[1], Ion-Daniel DIȚOIU[2], Laura Nicoleta ENARU[3], Brândușa GHIBAN[4*]

This paper investigates the influence of different thermal aging treatments on the structural and mechanical characteristics of the 2017A aluminum alloy. Three types of treatments are applied, at 120ºC, 140°C and 190°C, with holding times at each temperature of 1 hour, 12 hours and 24 hours, respectively.

A structural characterization is performed including: the phase constitution of the alloy and the grain size according to ASTM E3, ASTM E 407, ASTM E 112 standards, using the Barker electrolytic reagent with a power of x100. The mechanical characteristics (tensile strength, yield strength, elongation, resilience, hardness and microhardness) were determined. Finally, a fractographic analysis of the resilience fracture surfaces was performed.

Keywords: 2017A aluminum alloy; artificial aging; precipitation hardening; microstructural characterization; mechanical properties; fractographic analysis.

1. Introduction

Aluminum alloys have major advantages: a high specific modulus, good specific strength, superior corrosion resistance and better machinability. Due to this superior combination of properties compared to other alloys, they are now widely used in many industries, such as aerospace, automotive, high-speed rail engineering and others [1–3]. The strength and hardness of some metal alloys can be increased by the formation of extremely small, uniformly dispersed particles belonging to a second phase within the matrix. These result from subjecting the part to a heat treatment cycle known as precipitation hardening or “aging”, a name that comes from the fact that the process develops over time [4–9]. In the case of aluminum alloys, to improve their performance, these hardening phases (precipitates) must be

[1] Eng., Department of Metallic Materials Science and Physical Metallurgy, NUST POLITEHNICA Bucharest, Romania, e-mail buzatuandreead@yahoo.com
[2] Eng., Department of Metallic Materials Science and Physical Metallurgy, NUST POLITEHNICA Bucharest, Romania, e-mail ion_daniel.ditoiu@stud.sim.upb.ro
[3] Eng., Department of Metallic Materials Science and Physical Metallurgy, NUST POLITEHNICA Bucharest, Romania, e-mail laura.enaru@stud.sim.upb.ro
[4] * Prof., Department of Metallic Materials Science and Physical Metallurgy, NUST POLITEHNICA Bucharest, Romania, corresponding author, e-mail ghibanbrandusa@yahoo.com

thermodynamically stable and resist the coalescence process at the temperature of interest. This is achieved when the hardening precipitates are coherent and coplanar with the matrix, thus ensuring microstructural stability [10]. The strength of aluminum alloys is due to the fact that the impurity atoms in solution produce a deformation of the dislocation network, blocking their movement, which leads to increased hardness and mechanical strength [11-14]. The paper aims to: prepare a complex structural analysis, which, by optical microscopy methods, allows the assessment of the structures resulting from the application of artificial aging thermal treatments to the 2017A aluminum alloy; prepare a characterization of the complete mechanical behavior of the 2017A alloy structures after the application of different artificial aging thermal treatments, by building comparative histograms by type of mechanical characteristic; evaluation of the fracture surfaces of Charpy KCV impact specimens through stereomacrostructural analysis, with the possibility of identifying impact fracture mechanisms.

2. Research material and methodology

The 2017A aluminum alloy samples were taken from 30mm thick aluminum alloy sheet from COLOR METALS S.R.L, having the chemical composition indicated in Table 1. The chemical composition of the metallic material was determined by spectral analysis. For the experimental investigations of the present work, samples in the rolled state, T451 state, respectively solution hardening at 504°C, holding for 3-4 hours, with cooling in water, followed by natural aging at room temperature (20-25) °C for a minimum of (5-6) days were used.

Table 1

Chemical composition of experimental samples

Alloy	Chemical composition, %gr										
	Si	Fe	Cu	Mn	Mg	Cr	Zn	Ti	Zr	Pb	Al
Experimental	0.68	0.3	0,09	0.62	0,86	0.17	0,088	0.2	0.023	0.15	rest
EN AW-2017A	0.4	0.5	0,1	0.4-1,0	0,6-1,2	0,18-0,28	0,2	0.2	-	-	rest

The macroscopic aspects of the experimental specimens are shown in the image in Fig. 1.

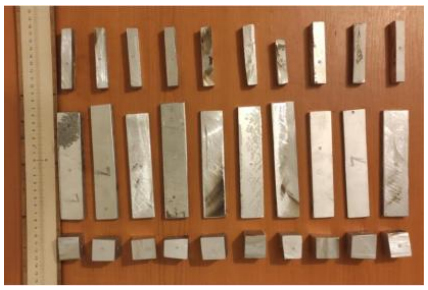

Fig. 1. Image of the macroscopic appearance of experimental specimens of alloy 2017A, with different dimensions for conducting experimental research

Experimental samples of alloy 2017A in rolled state T451 were subjected to different artificial aging heat treatments at 120ºC, 140°C and 190°C, with holding at each temperature for 1 hour, 12 hours and 24 hours, respectively.

The heat treatments were performed in a Nabertherm furnace at the Laboratory of Metallic Materials Science and the Physical Metallurgy Section of the Politehnica University of Science and Technology of Bucharest. Each type of heat treatment was tested six times to evaluate the mechanical properties: tensile strength, yield strength, elongation, resilience, hardness and microhardness. The grain size was determined according to ASTM E3, ASTM E 407, ASTM E 112 standards, using Barker electrolytic reagent with a power of x100. Structural analyses were performed with an OLYMPUS microscope.

The determination of the mechanical characteristics of the samples that were heat-treated by aging was done using a Walter + Bai AD universal testing machine from Switzerland, model LFV 300. The impact resistance test was performed by measuring the KCV values using a Walter Bai Pendulum Charpy hammer with a capacity of 300J.

The large-scale structural analysis was performed on an OLYMPUS SZX stereomicroscope, which was equipped with QuickMicroPhoto 2.2 software, and the small-scale analysis was performed on an OLYMPUS optical microscope, with Image Pro Plus software.

3. Experimental results and their interpretation

3.1 Structural characterization of alloy 2017A

The complete characterization of any metallic material begins with the analysis of the phase and constitutional structure of the respective material. The 2017A aluminum alloy is part of the 2xxx series of these material classes, consisting mainly of aluminum and copper, in the presence of various alloying elements, such as silicon, iron, manganese, magnesium, in low proportions of up to 1%. The main phase of this alloy is the solid solution of copper in aluminum, and the hardening phase is Al_2Cu. The results of the quantitative and qualitative visual metallographic analysis are shown in Fig. 2 – Fig. 11, both for the untreated alloy, in the T451

condition, and for the alloy subjected to various thermal aging treatments. Thus, the structure of the 2017A alloy, T451 state, is represented in Fig. 2, at different magnifications of the microscope. At a magnification of x100, Fig. 2(a), a structure consisting of solid solution is highlighted, with elongated grains and Al_2Cu-type precipitates, both in and intergranular, finely and uniformly distributed in the matrix. At higher magnifications (respectively x200, Fig. 2(b), or x500, Fig. 2(c)) these Al_2Cu precipitates can be quantitatively assessed as having a diameter of 1-3µm. When applying the aging treatment at 120°C /1h, Fig. 3, the structure does not change significantly, the precipitates being of the same size. When increasing the holding time at 120°C, respectively at 12h, Fig. 2, the precipitates agglomerate and grow to 5 µm (Fig. 4(c)). At a longer holding time at 120°C, respectively 24h (Fig. 5), the Al_2Cu precipitates increase in size, 5-6 µm (Fig. 5(c)). When applying an aging treatment at 140°C (Fig. 6 - Fig. 8) a slight increase in grain size and precipitates that increase as the holding time increases is noted. Thus, at 140°C/1h the Al_2Cu precipitates have dimensions of up to 10 µm (Fig. 6(c)) and reach about 10-12 µm at 140°C/24h (Fig. 8). Similar structures, namely solid solution of copper in aluminum and precipitates of Al_2Cu are also found when applying the aging treatment at 190°C, different holding times, Fig. 9 - Fig. 11. The precipitation of Al_2Cu particles is more abundant, as the holding time increases, respectively 1h, 12h and 24h. The size of the Al_2Cu particles is about 8-10 µm (Fig. 9 (c), Fig. 10 (c) and Fig. 11 (c)).

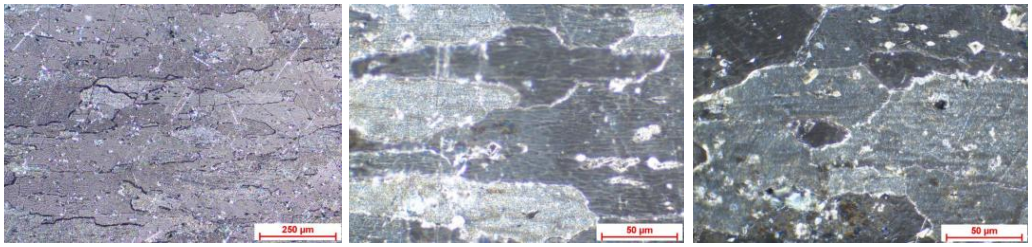

(a) (b) (c)

Fig. 2. Microstructural appearance of alloy 2017A, T451 condition, without aging heat treatment, at different microscope magnifications: (a) x100; (b) x500; (c) x1000

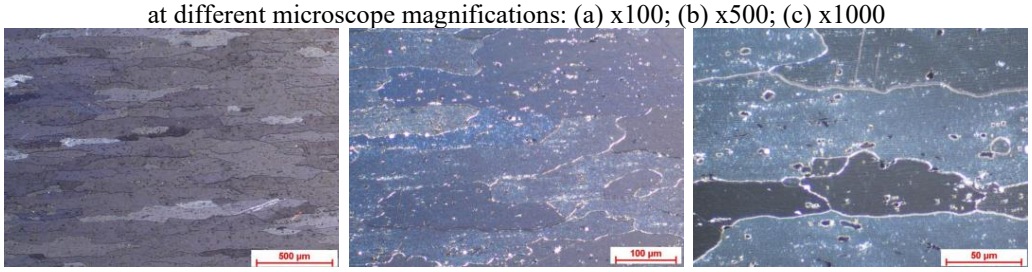

(a) (b) (c)

Fig. 3. Microstructural appearance of alloy 2017A, T451 condition + aging heat treatment at 120°C/1h, at different microscope magnifications: (a) x100; (b) x200; (c) x500

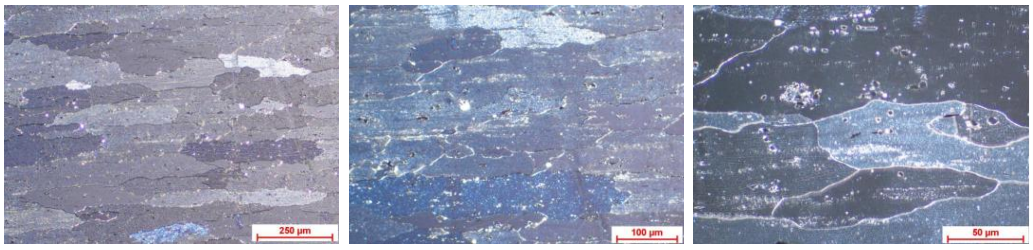

(a) (b) (c)

Fig. 4. Microstructural appearance of alloy 2017A, T451 condition + aging heat treatment at 120°C/12h, at different microscope magnifications: (a) x100; (b) x200; (c) x500

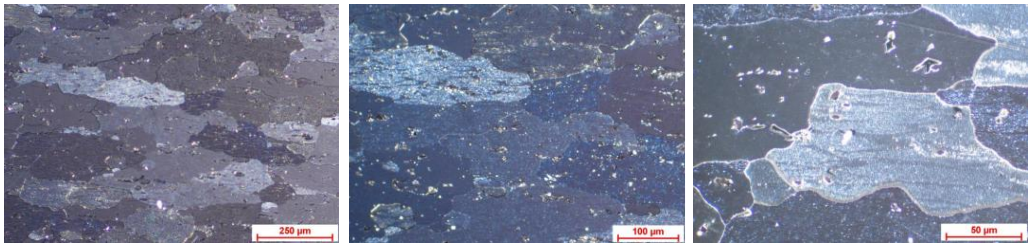

(a) (b) (c)

Fig. 5. Microstructural appearance of alloy 2017A, T451 condition + aging heat treatment at 120°C/24h, at different microscope magnifications: (a) x100; (b) x200; (c) x500

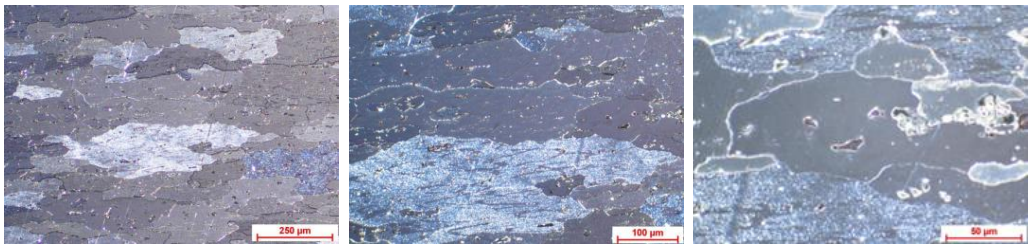

(a) (b) (c)

Fig. 6. Microstructural appearance of alloy 2017A, T451 condition + aging heat treatment at 140°C/1h, at different microscope magnifications: (a) x100; (b) x200; (c) x500

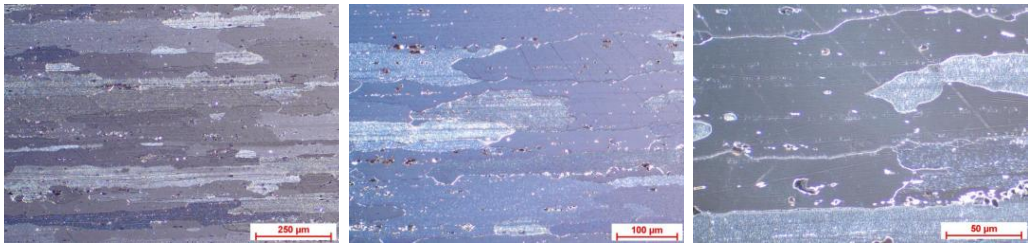

a b c

Fig. 7. Microstructural appearance of alloy 2017A, T451 condition + aging heat treatment at 140°C/12h, at different microscope magnifications: (a) x100; (b) x200; (c) x500

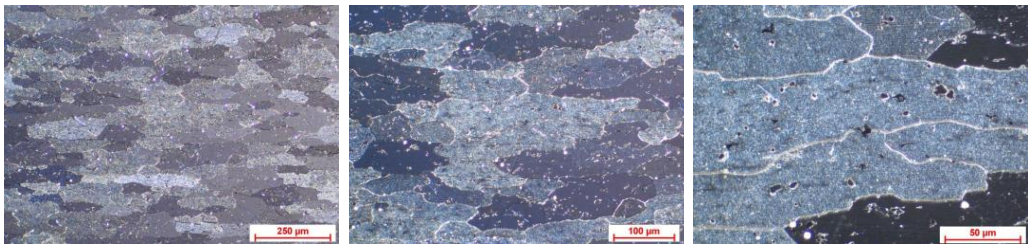

a b c

Fig. 8. Microstructural appearance of alloy 2017A, T451 condition + aging heat treatment at 140°C/24h, at different microscope magnifications: (a) x100; (b) x200; (c) x500

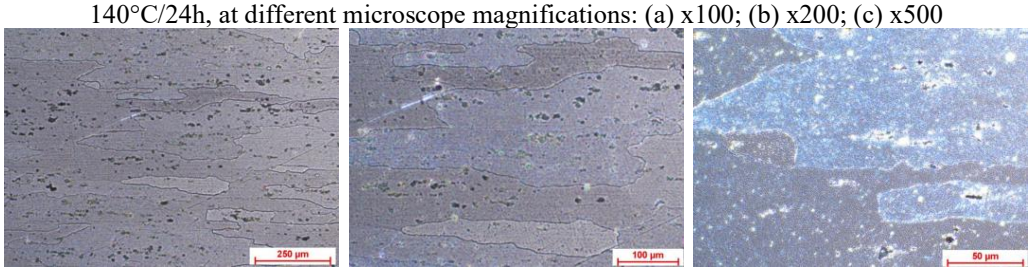

a b c

Fig. 9. Microstructural appearance of alloy 2017A, T451 condition + aging heat treatment at 190°C/1h, at different microscope magnifications: (a) x100; (b) x200; (c) x500

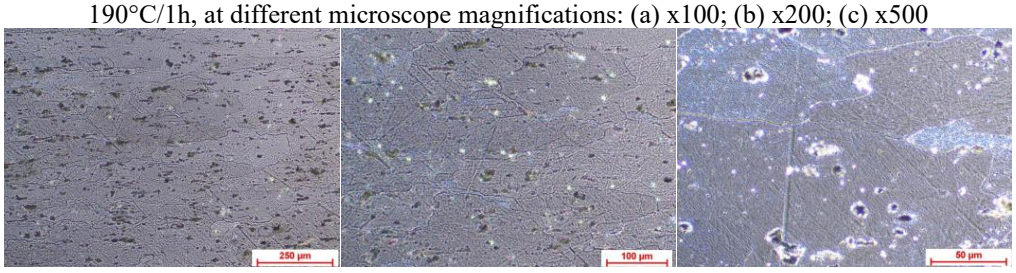

a b c

Fig. 10. Microstructural appearance of alloy 2017A, T451 condition + aging heat treatment at 190°C/12h, at different microscope magnifications: (a) x100; (b) x200; (c) x500

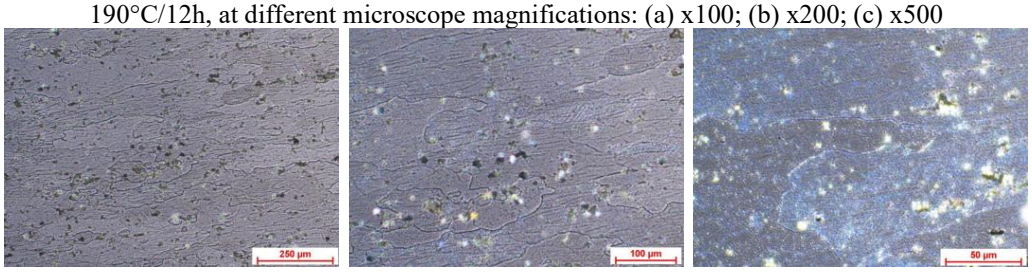

a b c

Fig. 11. Microstructural appearance of alloy 2017A, T451 condition + aging heat treatment at 190°C/24h, at different microscope magnifications: (a) x100; (b) x200; (c) x500

3.2 Determination of the grain size of alloy 2017A, in different structural states

Grain size is an important parameter in the structural characterization of a metallic material, providing the possibility of its complete evaluation. The method

by which the grain size was determined was by quantitative metallographic analysis according to ASTM E3, ASTM E 407, PO-043, PO-042, PO-044, using Barker reagent, at an examination at x100. The results regarding the determination of the grain size of the experimental specimens after applying different thermal aging treatments are shown in Fig. 12 - Fig. 21 and summarized in Table 2.

The following conclusions regarding the analysis of grain size values should be noted: The average grain size with the highest value is recorded in the control sample, not heat-treated, with an average grain size of 193 μm, falling into class 4, according to ASTM E112. In the samples heat-treated at 120°C, the grain size falls into class 5.5 according to ASTM E112, with the mention that the value decreases as the holding time increases, respectively from 173 μm (at 1h), to 115 μm (at 12h), reaching 120 μm (at 24h). In the samples heat-treated at 140°C, with different holding times, grain size values are recorded in the range of 93-124 μm, with the same mention that the value decreases as the holding time increases, falling into class 5.5 according to ASTM E112. In the samples heat-treated at 190°C, with different holding times, the lowest grain size values are recorded in the range of 92-121 μm, falling into class 5.5-6, according to ASTM E112. The histogram in Fig. 22, gives a synthetic representation of the results regarding the determination of grain size, allowing their comparison.

Table 2

Determination of grain size of experimental aluminum alloy 2017A

State	Grain size				
	Minimum, μm	Maxim, μm	Average, μm	Standard deviation, μm	ASTM Class E112
T451, martor (UM)	1,045	530	193	115	4
T451+ 120°C/1h	2,111	765	173	131	5,5
4T51+ 120°C/12h	4,379	552	115	107	5,5
T451+ 120°C/24h	1,045	584	120	118	5,5
T451+ 140°C/1h	1,058	349	124	70	5,5
T451+ 140°C/12h	2,091	660	115	116	5,5
T451+ 140°C/24h	0,548	362	93	66	6
T451+ 190°C/1h	1,045	456	121	106	5,5
T451+ 190°C/12h	1,043	259	97	62	6
T451+ 190°C/24h	1,045	641	92	93	6

The analysis of the results from the histogram of grain size values of the 2017A aluminum alloy specimens in different structural states (Fig. 22) allows the formulation of the following observations: By applying the aging heat treatments, the grain size is reduced, regardless of the temperature or holding time applied, respectively it is traced from class 4 (for the control specimen) to classes 5, or even 5.5 according to ASTM E112 for heat treated specimens; The smallest grain size

values are recorded for the specimens heat treated by aging at 190°C, with fine grains that fall into class 6, according to ASTM E112, compared to the grains in class 4, corresponding to the sample in the T451 delivery state, not heat treated.

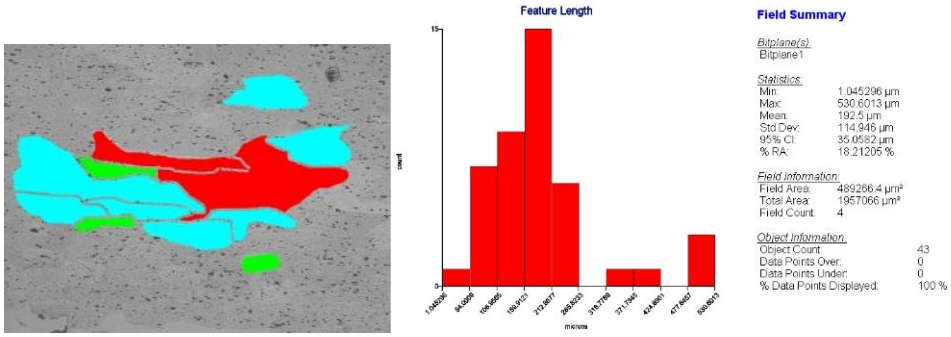

(a) (b)

Fig. 12. Determination of the grain size of alloy 2017A, condition 451, control sample: (a) analyzed image, (b) statistical analysis

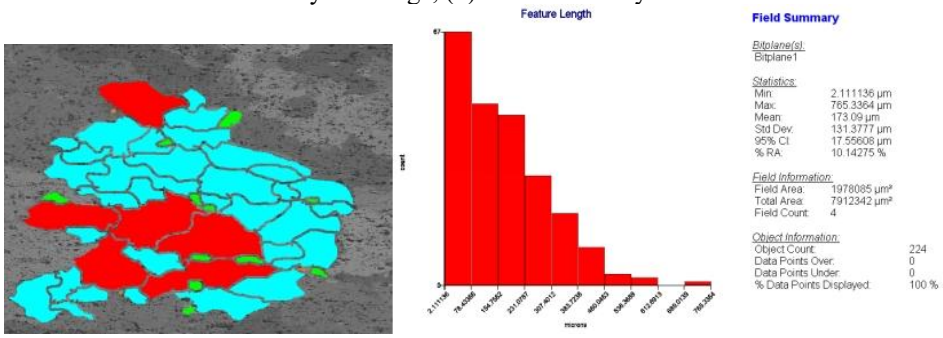

(a) (b)

Fig. 13. Determination of the grain size of alloy 2017A, condition 451+ artificial aging at 120°C/1h: (a) analyzed image, (b) statistical analysis

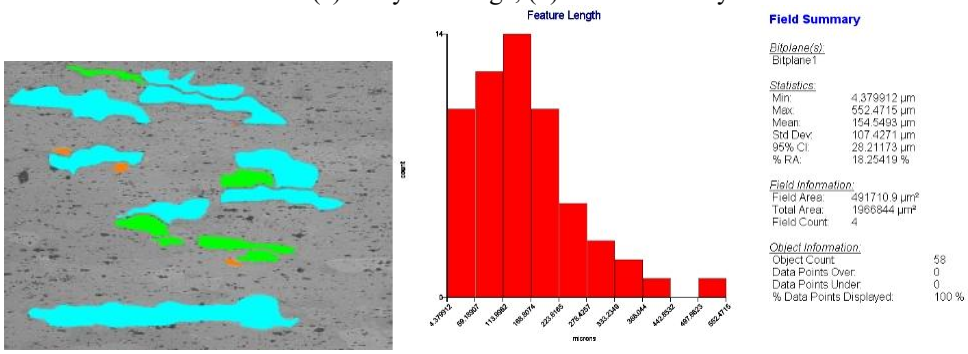

(a) (b)

Fig. 14. Determination of the grain size of alloy 2017A, condition 451+ artificial aging at 120°C/12h: (a) analyzed image, (b) statistical analysis

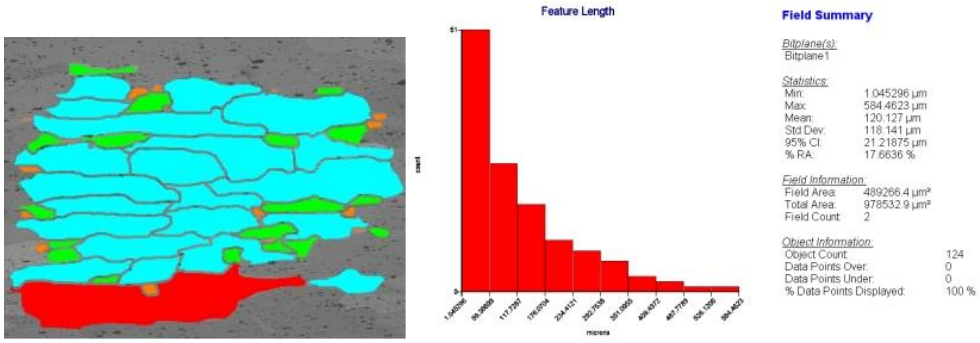

(a) (b)

Fig. 15. Determination of the grain size of alloy 2017A, condition 451 + artificial aging at 120ºC/24h/air: (a) analyzed image, (b) statistical analysis

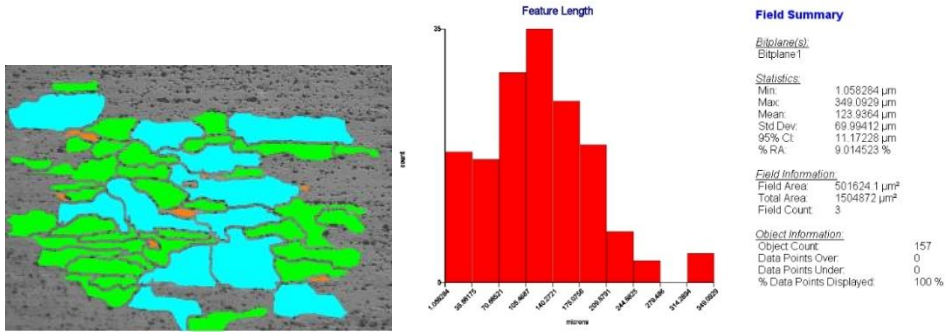

(a) (b)

Fig. 16. Determination of the grain size of alloy 2017A, condition 451 + artificial aging at 140ºC/1h/air: (a) analyzed image, (b) statistical analysis

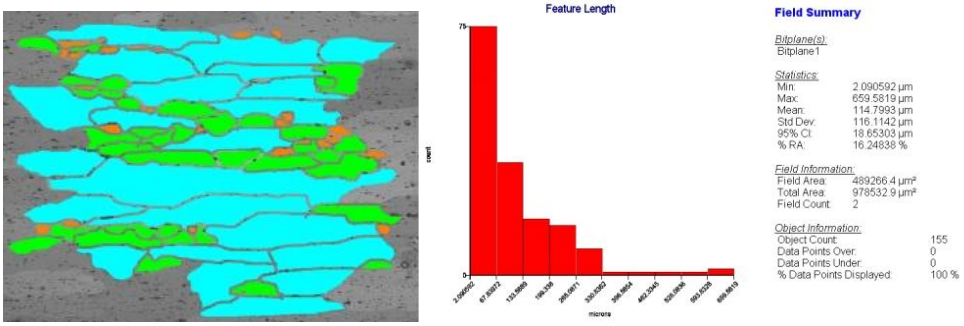

(a) (b)

Fig. 17. Determination of the grain size of alloy 2017A, condition 451 + artificial aging at 140ºC/12h/air: (a) analyzed image, (b) statistical analysis

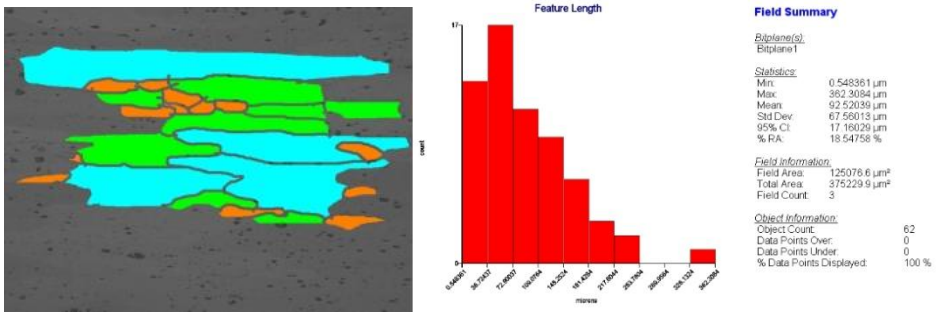

(a) (b)

Fig. 18. Determination of the grain size of alloy 2017A, condition 451 + artificial aging at 140ºC/24h/air: (a) analyzed image, (b) statistical analysis

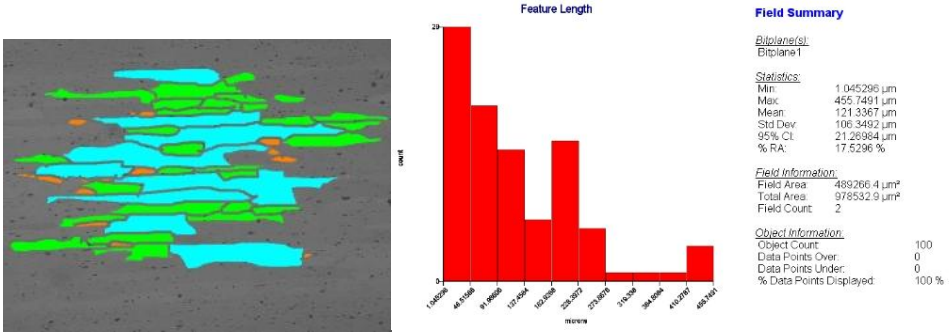

(a) (b)

Fig. 19. Determination of the grain size of alloy 2017a, condition 451 + artificial aging at 190ºC/1h/air: (a) analyzed image, (b) statistical analysis

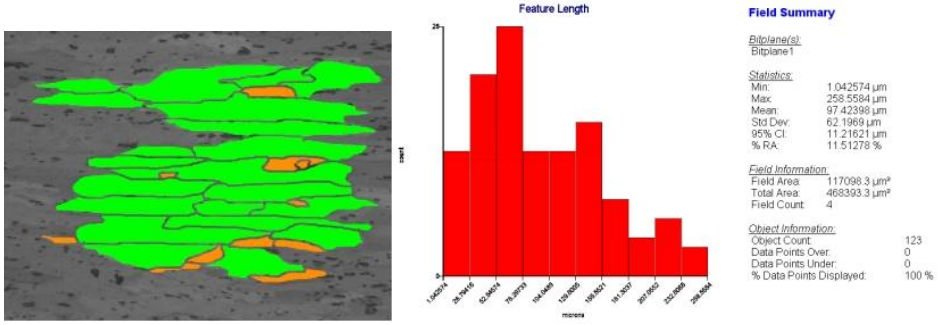

(a) (b)

Fig. 20. Determination of the grain size of alloy 2017a, condition 451 + artificial aging at 190ºC/12h/air: (a) analyzed image, (b) statistical analysis

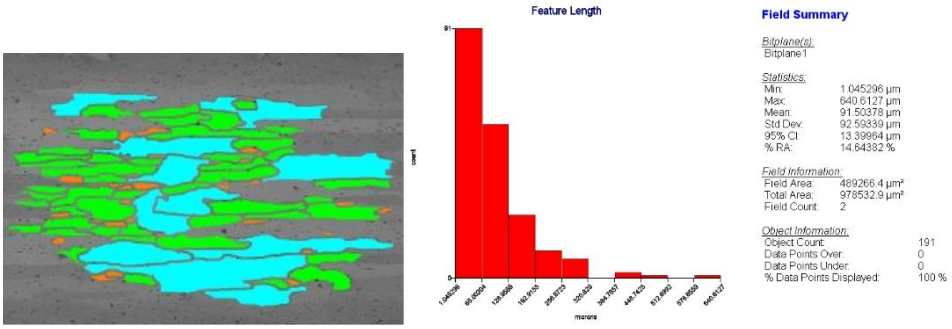

(a) (b)

Fig. 21. Determination of the grain size of alloy 2017a, condition 451 + artificial aging at 190ºC/24h/air: (a) analyzed image, (b) statistical analysis

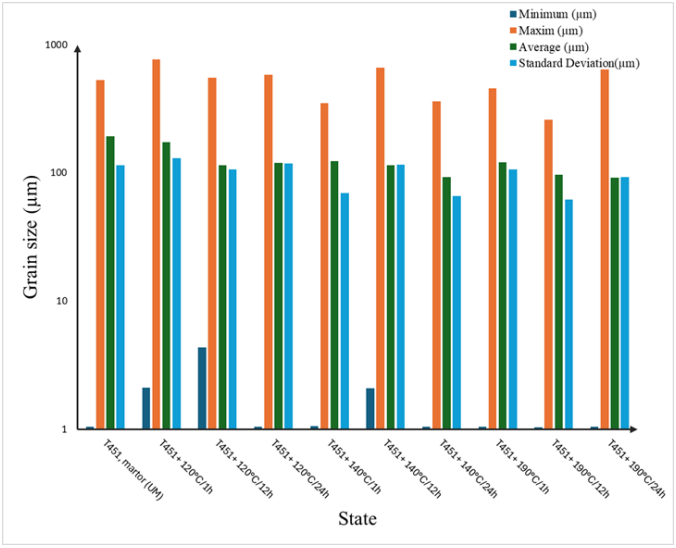

Fig. 12. Appearance of the histogram relating to grain size values for the experimental alloy 2017A in different heat treatment states

3.3 Determination of the mechanical characteristics of the experimental alloy 2017A

Mechanical behavior is very important in obtaining performance of the mechatronic material in service, so that the determination of the main mechanical characteristics becomes an important factor in the complete characterization of a material. Applying different heat treatments to aluminum alloys can cause drastic changes in mechanical characteristics and consequently can improve performance in service. Following the application of artificial aging heat treatments to the 2017A aluminum alloy, the following mechanical characteristics values were obtained, which after statistical processing were presented in the form of histograms, grouped by types of mechanical characteristics, as indicated in Fig. 23.

The variation of the values corresponding to the mechanical strength and yield strength of the 2017A aluminum alloy specimens in different structural states is shown in Fig. 23(a). A first remark refers to the fact that the application of different aging heat treatments does not substantially improve these mechanical characteristics. Thus, only aging at 120°C can increase the values of tensile strength by about 8-15%. The other aging temperatures cannot lead to an increase in the values of tensile strength. As for the values of the yield strengths, they are much reduced compared to those of the control specimen, a decrease of about 12-36% being observed. It is also noted that the holding time at each aging heat treatment temperature cannot be correlated with the value of either the mechanical strength or the yield strength. The variation of the necking and resilience values of the aged specimens of alloy 2017A in different structural states is illustrated in Fig. 23(b). The analysis of the necking values indicates that there is a slight increase only when aging at 120°C / 24 hours and at 190°C / 1h, otherwise at the other temperatures the necking values are much reduced compared to the control sample. Regarding the analysis of the resilience values, they are much reduced by applying the aging treatments at temperatures of 120°C, 140°C or 190°C. The variation of the microhardness and HBW hardness values is illustrated in Fig. 23(c)Regarding the analysis of the hardness values, it is found that after applying the aging thermal treatments, the material does not harden, possibly only aging at 120°C / 24 hours leads to the preservation of the value. Otherwise, at the other thermal treatments there is a drastic decrease in the hardness values, in the range of 9-38%. The analysis of the microhardness results highlights a minor hardening effect of the aging heat treatments, in a small range of 2-4%. Moreover, this analysis is not conclusive at the macroscopic scale, because at a local level, there is the probability of obtaining results that cannot be compared due to the positioning on the hardening particle or on the matrix of the penetrator.

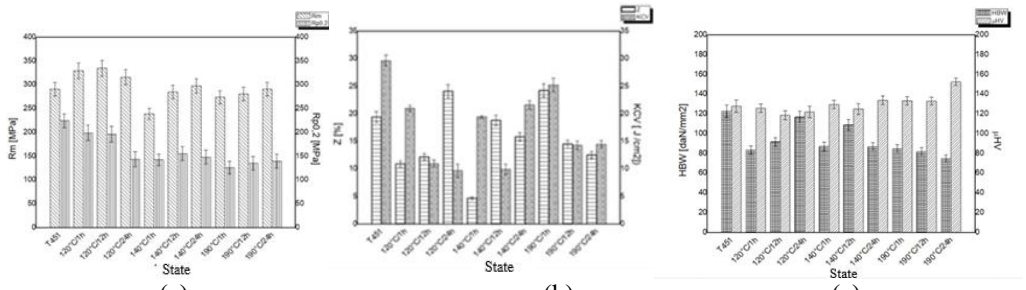

(a) (b) (c)

Fig. 23. Appearance of the histograms of the tensile strength and yield strength of alloy 2017A (a), necking and resilience (b) and HBW hardness and HV microhardness (c) of the control sample and the specimens heat-treated by aging at 120°C, 140°C and 190°C

As a general conclusion, it is found that by applying thermal aging treatments at 120ºC, 140ºC or 190ºC with different holding times (1h, 12h or 24h)

the values of tensile strength, necking and microhardness increase. Thus, an increase of about 15% in tensile strength compared to the untreated specimen after 120°C/12h/water and an increase of about 26% in necking (at 120°C/24h/water) is noted. Also, the hardening phases produce an increase of microhardness by about 19% (at 190°C/24h/water). Finally, the mechanical properties and grain size of 2017 aluminum alloy (a high-strength Al-Cu-Mg "duralumin" alloy) are critical in determining its suitability for high-performance applications like aircraft structures, rivets, and precision machined parts.The alloy's performance is driven by a combination of high strength (approx. 500 MPa tensile strength), good machinability, and, notably, high fatigue resistance. According to the Hall-Petch relationship, fine grains significantly increase the yield strength and hardness of 2017 alloy. Fine-grained 2017 is essential for high-load, safety-critical parts where sudden yield is unacceptable. While refining the grain structure enhances strength, it often improves ductility, which is critical for forming and shaping 2017 alloy during manufacturing. Finer grain structures reduce the likelihood of casting defects, such as porosity and compositional segregation (common issues in 2017 alloy). Although finer grains can increase corrosion resistance by reducing the size of precipitates, it also increases the total grain boundary area, which can have complex effects on corrosion behavior. However, generally, refined, uniform equiaxed grains improve overall performance.

3.4 Stereo macrostructural analysis of resilience specimens of 2017A specimens in different structural states of aging heat treatment

A fractographic analysis of the fracture surfaces of Charpy KCV impact indentations was performed using a stereomicroscope, at the macroscopic scale, as a novelty of this work. The main structural elements of the dynamic impact fracture were identified, and at the same time, the elements that can differentiate the propagation mode of the fracture generated by the application of different thermal aging treatments were identified. The samples corresponding to the holding times of 1h, 12h and 24h were analyzed macroscopically, for each aging heat treatment temperature, respectively 120°C, 140°C and 190°C. The results of the fractographic analysis of the impact fracture surfaces on Charpy KCV resilience specimens are shown in Fig. 24 – Fig. 27. It is noted that the fracture is dynamic in nature, with a fibrous appearance, and the propagation mode of the fracture front is different, depending on the aging treatment applied. The fracture surface of the control specimen, in the T451 condition, without the application of an aging heat treatment is shown in Fig. 24. A rough surface, with a fibrous appearance, with zig-zag propagation of the fracture front is noted. The macroscopic appearance of the fracture surfaces of the specimens heat-treated at 120°C, different holding times is shown in Fig. 25. The same fibrous appearance of the surfaces in cross-section is noted, unlike the control sample in terms of the propagation of the fracture front,

following a curved line. No differences in the fractographic aspects are noted due to the different holding times, respectively 1h, 12h or 24h, all specimens having similar fractographic aspects. The macroscopic appearance of the fracture surfaces of the specimens heat-treated at 140°C, different holding times is shown in Fig. 26, being similar to that of the specimens after applying the aging treatment at 120°C. The same fibrous appearance of the surfaces in cross-section is noted, unlike the control sample in terms of the propagation of the fracture front, following a curved line. No differences in the fractographic aspects are observed due to the different holding times, respectively 1h, 12h or 24h, all the samples having similar fractographic aspects. The macroscopic aspect of the fracture surfaces of the heat-treated samples at 190°C, different holding times is shown in Fig. 27. The fractographic aspects of these samples, both in cross-section and frontal, are different from those of the control sample (Fig. 24), as well as from those of the samples heat-treated at 120°C (Fig. 25) or 140°C (Fig. 26).

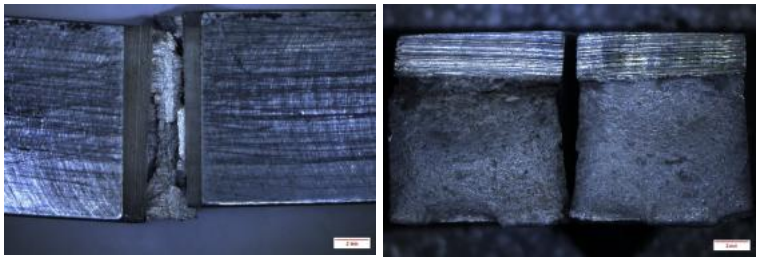

(a) (b)

Fig. 24. Fractographic appearance of the fracture surfaces of the impact specimens for alloy 2017, condition T451 (control sample, Z): (a) longitudinal section; (b) transverse section

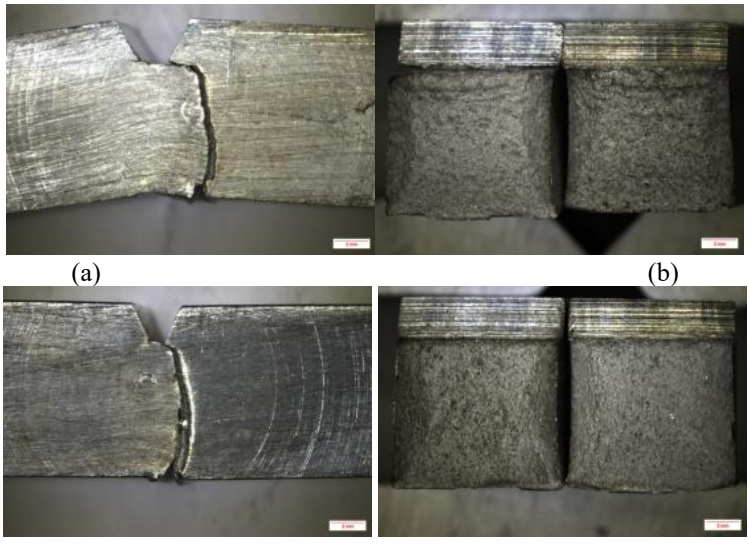

(a) (b)

(c) (d)

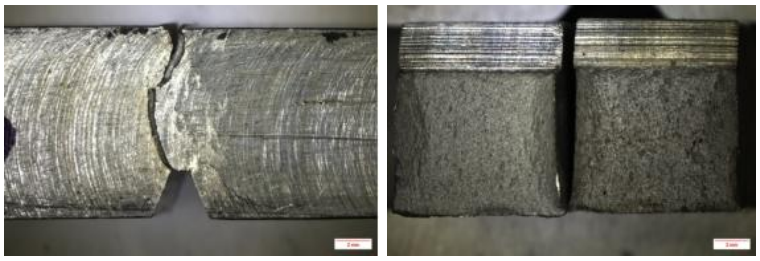

(e) (f)

Fig. 25. Fractographic appearance of the fracture surfaces of the impact specimens for alloy 2017, T451 condition + artificial aging at 120°C, different holding times: (a,b) - 1 hour; (c,d)- 12 hours; (e,f) - 24 hours; and different sections: (a, c, e) - longitudinal; (b,d,f) – transverse

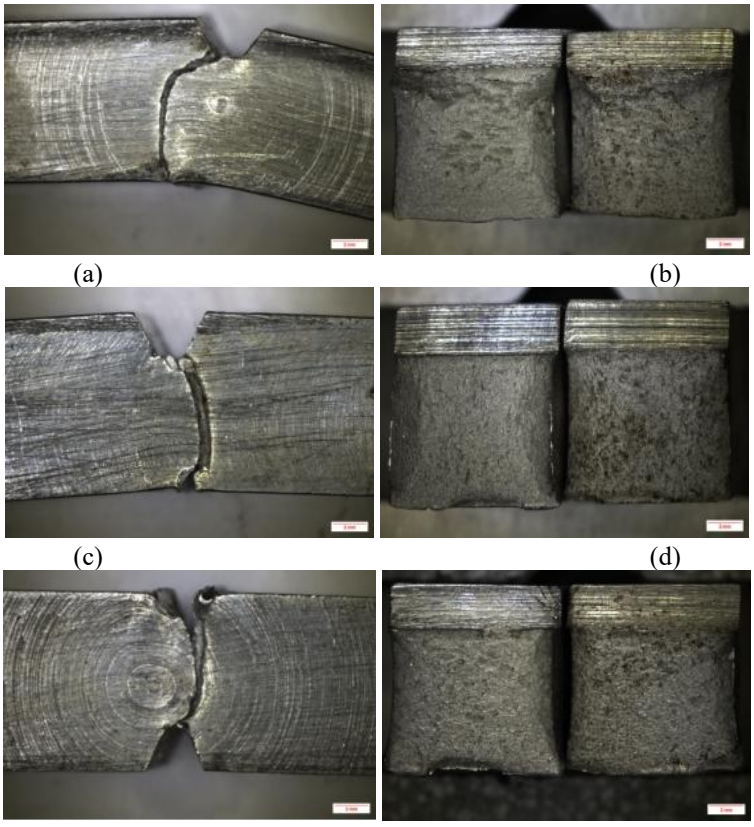

(a) (b)

(c) (d)

(e) (f)

Fig. 26. Fractographic appearance of the fracture surfaces of the impact specimens for alloy 2017, T451 condition + artificial aging at 140°C, different holding times: (a,b) - 1 hour; (c,d)- 12 hours; (e,f) - 24 hours; and different sections: (a, c, e) - longitudinal; (b,d,f) - transverse

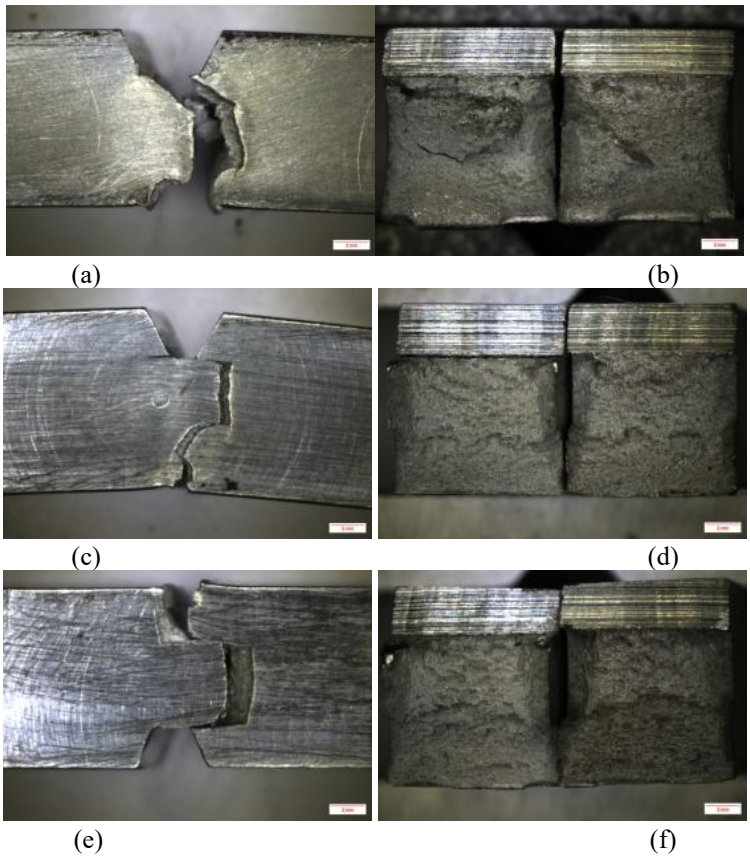

Fig. 27. Fractographic appearance of the fracture surfaces of the impact specimens for alloy 2017, T451 condition + artificial aging at 190°C, different holding times: (a,b) - 1 hour; (c,d)- 12 hours; (e,f) - 24 hours; and different sections: (a, c, e) - longitudinal; (b,d,f) – transverse

Thus, the fibrous aspects of the surfaces in cross-section appear with material tearing, the propagation of the fracture front taking place in a zigzag pattern, with strong deformation of the section edges. Also, no differences in fractographic aspects are observed due to different holding times, respectively 1h, 12h or 24h, all samples treated at 190°C having similar fractographic aspects.

4. Conclusions

The structural and mechanical investigations carried out in this work led to the following observations. Structural analysis revealed a structure consisting of solid solution α, with elongated grains and precipitates of the Al_2Cu type, intra and intergranular, finely and uniformly distributed in the matrix. The differences in the aging structures consist either in the modification of the size of the precipitation particles, or in their distribution in the solid solution α. Thus, the precipitates agglomerate and grow up to 5μm (at 120ºC/1 hour/water), their size reaching up to 5-6μm (at 120ºC/1 hour/water); when applying an aging treatment at 140°C, a slight

increase in granulation and precipitates is noted that grow as the holding time increases, reaching 10-12µm (140°C/24h/water); when applying the aging treatment at 190°, the precipitation of Al_2Cu particles is more abundant, reaching about 8-10µm (190ºC/24h/water). By applying aging heat treatments to alloy 2017A, T451 condition, the grain size is refined, from an average grain size of 193µm to 92µm (after 190ºC/24h/water). By applying thermal aging treatments, it is found that by applying thermal aging treatments at 120ºC, 140ºC or 190ºC with different holding times (1h, 12h or 24h) the values of tensile strength, necking and microhardness increase. Thus, an increase of about 15% in tensile strength compared to the untreated sample (at 120°C/12h/water) and an increase of about 26% in necking (at 120°C/24h/water) is noted. Also, the hardening phases produce an increase of microhardness by about 19% (at 190°C/24h/water).

REFERENCES

[1] *T. Sato*, Innovative development of aluminum research and technologies in Japan, in Proceedings of the 12th International Conference on Aluminum Alloys, Yokohama, Japan, September 5–9, 2010, Japan Institute of Light Metals, Tokyo, 2010.

[2] *Q. Liu, L. Lin,* Current status of research and industries of Al sheets in China, in Proceedings of the 12th International Conference on Aluminum Alloys, Yokohama, Japan, September 5–9, 2010, Japan Institute of Light Metals, Tokyo, 2010, pp. 20–29.

[3] *J. Hirsch, H. I. Laukli*, Aluminum in innovative light-weight car design, in Proceedings of the 12th International Conference on Aluminum Alloys, Yokohama, Japan, September 5–9, 2010, Japan Institute of Light Metals, Tokyo, 2010, pp. 46–53.

[4] *W. F. Smith*, Fundamentos de la Ciencia e Ingeniería de Materiales, 3rd ed., McGraw-Hill Interamericana, España, 1998.

[5] *D. R. Askeland*, La Ciencia e Ingeniería de los Materiales, Grupo Editorial Iberoamérica.

[6] *R. E. Reed-Hill*, Principios de Metalurgia Física, 2nd ed., Compañía Editorial Continental, México, 1971.

[7] *D. A. Porter, K. E. Easterling,* Phase Transformations in Metals and Alloys, Van Nostrand Reinhold, UK, 1984.

[8] *P. G. Shewmon*, Transformations in Metals, McGraw-Hill Book Company, USA, 1969.

[9] American Society for Metals, Metals Handbook, **Vol. 2**, 8th ed., ASM International, Metals Park, OH, 1973, pp. 271–283.

[10] *Q. Li, F. E. Warner*, Characterization of a cubic phase in an Al-Cu-Mg-Ag alloy, Journal of Materials Science, **Vol. 32**, 1991, pp. 301–309.

[11] *W. Callister,* Introducción a la ciencia e ingeniería de los materiales, 3rd ed., Ed. Reverté, Barcelona, España, 2001, pp. 74, 349–355, 375–378.

[12] *J. D. Robson et al.,* Advances in microstructural understanding of wrought aluminum alloys, Metallurgical and Materials Transactions A, **Vol. 51A**, 2020, 4377.

[13] *A. Khalfallah, A. Raho, S. Amzert, A. Djemli,* Precipitation kinetics of GP zones, metastable η′ phase and equilibrium η phase in Al–5.46 wt% Zn–1.67 wt% Mg alloy, Transactions of Nonferrous Metals Society of China, **Vol. 29**, No. 2, 2019, pp. 233–241.

[14] *Y. S. Lee, D. H. Koh, H. W. Kim, Y. S. Ahn,* Improved bake-hardening response of Al–Zn–Mg–Cu alloy through pre-aging treatment, Scripta Materialia.